Circular Dichroism Spectroscopy by Four-Wave Mixing Using Polarization Grating-Induced Thermal Gratings

Jon A. Nunes and William G. Tong*

Department of Chemistry, San Diego State University, San Diego, California 92182

David W. Chandler and Larry A. Rahn

Combustion Research Facility, Sandia National Laboratories, Livermore, California 94551

Received: November 15, 1996; In Final Form: February 27, 1997[⊗]

A novel four-wave mixing technique for the measurement of circular dichroism in optically active liquid samples is demonstrated. When two cross-polarized continuous-wave laser beams are crossed at a small angle in a circular dichroic liquid, a weak thermal grating is produced with a phase depending on the sign of the circular dichroism. The polarization of one of the beams can be modified to allow coherent interference with an intensity grating-induced thermal grating. A probe beam scattering from the composite grating results in a coherent signal beam that reveals the sign and the magnitude of analyte circular dichroism. The use of this technique to optimize the signal-to-noise ratio in the presence of scattered light and laser noise is discussed.

Introduction

The laser has played a revolutionary role in the advancement and the development of modern optical diagnostic methods. It has improved many conventional techniques, while aiding in the creation of entirely new diagnostic practices that are only possible using the laser light. An important example of a new technique is four-wave mixing (FWM), also commonly referred to as laser-induced grating spectroscopy (LIGS).[1] Four-wave mixing has proven to be a powerful tool for probing the chemical and physical properties of numerous different sample types. A particularly useful technique is degenerate four-wave mixing (DFWM) which has been demonstrated as a sensitive analytical spectroscopic method[2] in many different environments, including low-pressure hollow-cathode discharge cells,[3−5] flame atomizers,[6−9] and liquid flow cells.[10,11] In the gas phase, sub-Doppler spectral resolution allows hyperfine structure measurement and stable isotope ratio analysis at trace concentration levels.[9] For condensed-phase analytes, attomole-level detection sensitivity has been obtained using continuously flowing liquid cells.[12] Two-color variants of DFWM have been used for gas-phase excited-state spectroscopy,[13,14] for measurements of small absorptions in liquids,[15,16] and for the study of molecules in free-jet expansions.[17] These methods offer unique advantages over many conventional optical spectroscopic techniques including excellent laser-limited spectral resolution, convenient and efficient optical signal collection on a virtually "zero" background, and excellent detection sensitivity.

Taking advantage of these unique features, Nunes and Tong[18] reported a DFWM technique to measure circular dichroism (CD), the differential absorption of right- and left-handed circularly polarized light that chiral molecules exhibit. Circular dichroism spectroscopy is an optical method for analyzing the chirality of molecules. It has become the method of choice[19] over polarimetry and optical rotary dispersion for the study of inorganic and organic molecular structural configurations,[20] the study of conformational properties of proteins,[21] and the analytical detection of optically active substances.[22−24] Nunes and Tong demonstrated the first CD measurements based on a forward scattering degenerate four-wave mixing (F-DFWM) geometry and were able to make sensitive CD measurements by employing a Pockels cell for polarization modulation.

In this paper we investigate the use of a continuous-wave laser-based four-wave mixing technique to detect circular dichroism of liquid samples using polarization gratings[25] in addition to thermal gratings. The DFWM signal is produced by scattering of a probe laser beam from the effects of a thermal grating in the sample induced by periodic variations in absorption in the intersection volume of two coherent excitation laser beams. When the excitation beams are of the same polarization, an intensity modulation is produced at their intersection, and any optical absorption results in a thermal grating. When the excitation beams are cross-polarized, however, only the polarization is modulated at their intersection, and there is normally no thermal grating produced. In samples that exhibit circular dichroism, a weak thermal grating is produced even with cross-polarized beams because the absorption is polarization dependent. Nonchiral samples do not produce such a signal. As described later, the polarization of one of the cross-polarized beams can be modified to allow coherent interference with an intensity-grating-induced thermal grating. A probe beam scattering from the composite grating results in a signal beam that reveals the sign and the magnitude of analyte circular dichroism. Recently, a pulsed laser cross-polarized LIGS experiment for CD detection was demonstrated in a letter by Terazima.[26] In our report, the use of a continuous-wave laser-based FWM technique to optimize the signal-to-noise ratio in the presence of scattered light and laser amplitude noise is discussed. The potential advantages of using a continuous-wave FWM technique to make CD measurements as compared to conventional CD methods and the potential applications for time-resolved CD spectroscopy using pulsed lasers are also discussed.

Background

Circular Dichroism. CD is defined as the difference in absorbance of left circularly polarized light (LCPL) and right circularly polarized light (RCPL). The absorption-based CD signal can be described in terms of molar absorptivities for LCPL and RCPL as

$$\Delta\epsilon = \epsilon_L - \epsilon_R \tag{1}$$

* Corresponding author.

[⊗] Abstract published in *Advance ACS Abstracts,* April 15, 1997.

S1089-5639(96)03813-3 CCC: $14.00

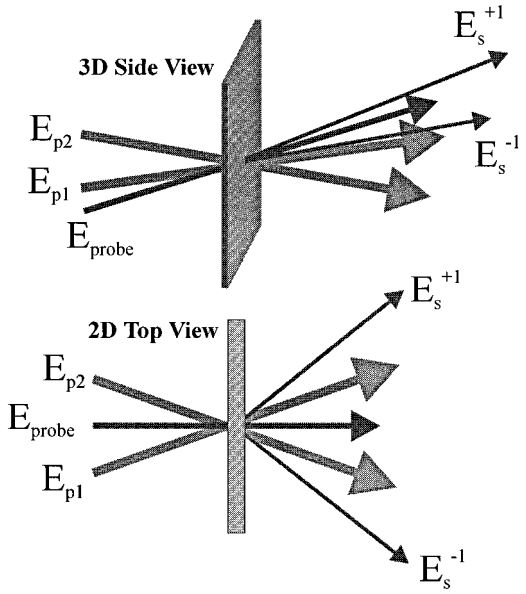

Figure 1. Two- and three-dimensional representations of the four-wave mixing geometry used in the experiment. The two pump waves, E_{p1} and E_{p2}, are in the same plane, and they have crossed polarizations with respect to one another. The thin grating scatters the probe beam E_{probe} into two signal beams, $E^{+1}{}_s$ and $E^{-1}{}_s$.

where ϵ_L and ϵ_R are the molar absorptivities for LCPL and RCPL, respectively, and $\Delta\epsilon$ is the differential molar absorptivity. Equation 1 can be related to conventional absorbance measurements by substitution into the Beer−Lambert law,

$$\Delta A = A_L - A_R = \Delta\epsilon bC = \epsilon_L bC - \epsilon_R bC \qquad (2)$$

where b is path length (cm), C is concentration (M), A_L and A_R are the absorbance for LCPL and RCPL, respectively, and ΔA is the differential absorbance.

Four-Wave Mixing. FWM is a process that can, among other ways, be described in terms of the creation and scattering from laser-induced gratings.[1] The spatially (and possibly temporally) modulated electric field resulting from the interference between two crossed excitation or pump beams affects the optical properties of a medium. A signal is generated when a third probe beam is diffracted from the modulation grating induced by the pump beams. This is especially useful in cases where thermal gratings are the important mechanism, as they are in the present work. The relation of the grating picture to that of the nonlinear optical susceptibility has been discussed by Meyers and Hochstrasser[27] and Fourkas et al.[28] Meyers and Hochstrasser reported time-resolved four-wave mixing experiments for the study of ground- and excited-state molecular rotational dynamics, where the induced optical anisotropy acts as a grating to diffract the probe pulse and create a signal pulse.[27] In this paper, we report a mechanism in which the signal component of interest results from a *thermal* grating that ordinarily does not exist using cross-polarized pump beams, unless the sample exhibits circular dichroism at the pump wavelength, as described below.

The experimental geometry used in this work is depicted in Figure 1. Two coherent excitation laser beams of wavelength λ_{ex} intersect at an angle α. The laser-induced grating modulation at the intersection is transverse to the excitation beams and has a spacing given by

$$d = \lambda_{ex}/2 \sin(\alpha/2) \qquad (3)$$

The direction of the probe laser is typically determined by phase-matching conditions. The path length through the sample cell is sufficiently short (i.e., 0.5 mm), and hence, the probe beam can be directed into the sample at any angle as long as it is overlapped with the grating excitation beams. This Raman−Nath or "thin-grating condition"[29] produces scattering of the probe beam into multiple diffraction orders, one of which is directed into the photodetector.

Thermal Grating. A thermal grating can be generated when two laser beams are crossed at a small angle inside an absorbing liquid. Crossed beams with the same linear polarizations create an intensity pattern (i.e., an intensity grating) in the crossover region of the two beams. The pattern resembles a conventional diffraction grating composed of light and dark interference fringes. This intensity modulation can be imprinted on the absorbing medium in the form of a thermal modulation or "thermal grating" that is spatially coherent with the intensity pattern. Absorption and subsequent radiationless relaxation in the sample produces a thermal grating with higher temperature fringes aligned with the higher intensity fringes in an intensity grating. The temperature fluctuations result in corresponding spatial modulations of refractive index which act as a phase grating.[1] It is this spatially nonuniform refractive index that scatters the impinging probe laser beam. This process for parallel polarizations is depicted in Figure 2a, where the top portion shows the resultant grating electric field and the bottom section represents the thermal response by the absorbing sample.

When the same crossed input beams have perpendicular linear polarizations, a very different situation arises. No longer can the two beams interfere to form an intensity pattern. Since there is no generated intensity pattern, there can be no intensity-grating-induced thermal grating. This is easily demonstrated experimentally by rotating the electric field polarization of one the pump beams in a thermal grating experiment by 90°. The observed scattering signal is completely quenched when the pump polarizations are exactly orthogonal.

CD-Induced Thermal Gratings. There is, however, a way in which cross-polarized laser beams can produce a thermal grating in a liquid that exhibits circular dichroism. The interference pattern shown at the top of Figure 2b describes how the resultant electric field in the pump beam crossover region changes in polarization, but not in magnitude across one grating fringe. The polarization changes from right circular to linear, then to left circular, back to linear (90° shifted), and back to right circular. In between these polarization states are the corresponding transitional elliptical polarizations.[28] Thus, a "polarization grating" superimposed upon an absorbing chiral compound exhibiting circular dichroism results in a thermal grating (Figure 2b, bottom) that is produced by the differential absorption of right and left circularly polarized light (CPL). This can be illustrated as follows. Consider an optically active sample that possesses a negative $\Delta\epsilon$ value; i.e., it absorbs RCPL more than LCPL. Figure 2b shows the difference in absorption across one grating fringe (i.e., from $x = 0$ to $x = d$), and it is apparent that at $x = 0$, where the electric field polarization is RCP, there is maximum absorption by the sample. At $x = d/2$, where the electric field polarization is LCP, there is a minimum in the sample absorption. Finally at $x = d$, the polarization is again RCP, and the sample absorption is again at its highest point. This differential absorption results in a nonuniform spatial temperature distribution, i.e., a thermal grating. This thermal grating, although weak, can still generate a relatively strong DFWM signal detectable with a photomultiplier tube.

Further study reveals that the polarization of one the beams can be modified to allow coherent interference of a CD-induced thermal grating (CDTG) with an intensity-grating-induced thermal grating (IGTG). It is important to note that a CD-

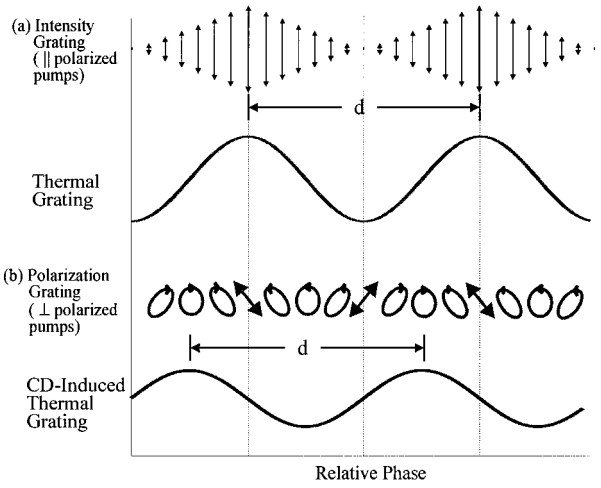

Figure 2. Relative phases of gratings relevant to this experiment. (a) Pump beams with parallel polarizations create an intensity grating; i.e., the resultant electric (top portion) field varies in intensity across the grating. In an absorbing medium, a thermal grating (lower) is formed. (b) Pump beams with crossed polarizations create a polarization grating where the resultant field varies in polarization, but not in intensity across the grating. In a chiral sample, this polarization grating gives rise to a CD-induced thermal grating where the grating peaks and troughs correspond to the different circular polarizations across the polarization grating fringes. Note that the intensity-induced thermal grating and the CD-induced thermal grating are 90° out of phase.

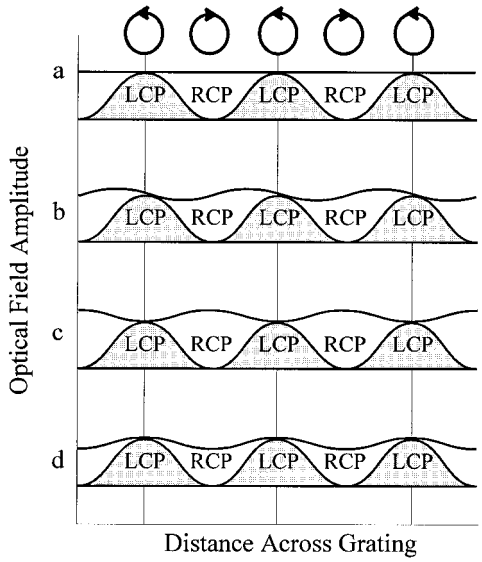

Figure 3. Phase representation of circular dichroism-induced thermal grating (CDTG) and intensity grating-induced thermal grating (IGTG) interference. (a) Polarization grating shown in an electric field representation with only the circular portions drawn (top) and an optical field representation (lower). (b) A normal (i.e., unshifted) intensity grating is 90° out of phase with the polarization grating. (c) A 90° phase-shifted intensity grating will produce a thermal grating that will interfere with a CDTG. A sample with a positive $\Delta\epsilon$ will result in a grating that destructively adds to the phase-shifted IGTG. A negative $\Delta\epsilon$ results in constructive interference. (d) An oppositely phase-shifted IGTG reverses the resulting interferences for the different samples.

induced thermal grating is 90° (i.e., $d/4$) spatially phase shifted relative to an intensity-grating-induced thermal grating as shown in Figure 2. The direction of the shift depends on the sign, positive or negative, of $\Delta\epsilon$ of the particular sample under investigation. If $\Delta\epsilon$ has a positive sign, the sample absorbs LCPL more than RCPL, and the absorption maxima will thus be at the LCP regions of the polarization grating. If $\Delta\epsilon$ is negative, the opposite is true. By introducing a 90° phase-shifted IGTG of the correct magnitude, it is possible to coherently interfere both thermal gratings in the sample.

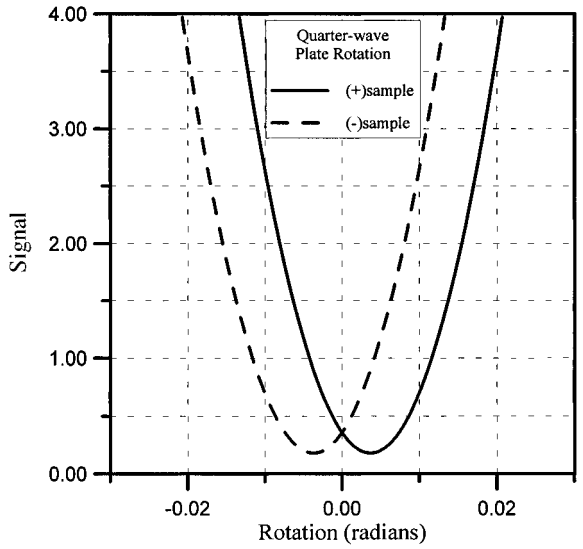

Figure 4. Theoretical plot of the average FWM signal vs quarter-wave plate rotation for a (+) and (−) chiral sample. Depending on the sign of the $\Delta\epsilon$ value, a minimum occurs in the signal when the rotation is at $\Theta = \Delta\epsilon/\epsilon$.

This process is schematically depicted in Figure 3. Two representations of a polarization grating are shown in Figure 3a. The top section is an electric field picture similar to that shown in Figure 2 with only the circular portions drawn, and below that is an optical field representation. The optical field drawing conveniently shows the spatial transition between the left and right circular polarizations across the grating. Figure 3b shows how the introduction of a normal (i.e., no phase shifted) IGTG is out of phase with the polarization grating. However, if an IGTG that is 90° phase shifted is added, as shown in Figure 3c, the two gratings are now correctly positioned to interfere. In a situation where a chiral substance that has a positive $\Delta\epsilon$ (i.e., more absorption of LCP than RCP) was under investigation, this IGTG would destructively interfere with the corresponding CDTG. If the correct amplitude of IGTG is added, a complete grating cancellation would occur, and the scattered signal will disappear. In the case of a chiral substance with a negative $\Delta\epsilon$, constructive interference occurs, causing the signal to increase in intensity. Figure 3d shows an IGTG profile for an opposite phase shift.

Experimentally, the described interference processes can be achieved by placing a quarter-wave retarder in one of the excitation pump beams and slightly rotating it. It can be shown[30] that this rotation is directly related to the ratio of the sample's circular dichroism ($\Delta\epsilon$) to the overall average absorption coefficient (ϵ) such that

$$Q = De/e \tag{4}$$

where Q (in radians) is the amount of quarter-wave plate rotation required to minimize the signal.

Figure 4 is a theoretical plot of the average signal vs rotation for a (+)/(−) chiral sample. Depending on the sign of $\Delta\epsilon$, a minimum occurs in the signal when the rotation is at $Q = \Delta\epsilon/\epsilon$. In the present work, these minima are experimentally determined for separate enantiomers of a chiral substance and compared to calculated values.

Experimental Section

The four-wave mixing experimental arrangement is shown in Figure 5. Gratings are formed using a single-mode CW argon

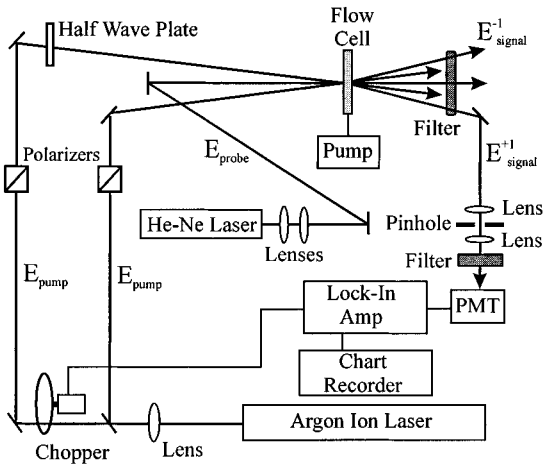

Figure 5. Four-wave mixing circular dichroism experimental setup.

ion laser (Spectra Physics, Model 171) operating at 488 nm. The laser output is split into two beams using a 50/50 beam splitter and recombined at the 0.5 mm path length liquid flow cell. One of the two pump beams passes through a mechanical chopper, operated at a frequency of 250 Hz that is part of the amplitude modulation scheme for lock-in detection of the signal, and then through a calcite polarizer to ensure "pure" linear polarization. The other beam passes through a calcite polarizer and a half-wave plate that is used to control the type of grating that is prepared in the sample solution. When the wave plate crystal axis is aligned with the beam polarization axis, there is no polarization rotation, and hence, both beams have parallel polarization. With this configuration an intensity grating is formed in the sample. When the wave plate is rotated 45°, the beams are cross-polarized and a polarization grating is generated.

A 1.5 mW He−Ne laser operating at 632 nm is used as the probe laser. The He−Ne probe beam is introduced below the plane occupied by the argon ion laser pump waves, and it is diffracted by the grating into two signal beams. One of the red-diffracted beams is passed through a blue color filter, a 250 mm pinhole, and a 632 nm laser line filter and finally directed to a PMT for detection. The amplitude modulated signal is sent to a lock-in amplifier that is frequency referenced to the mechanical chopper. The demodulated signal is recorded on a chart recorder and digitized by a personal computer.

Optically active (+)- and (−)-tris(ethylenediamine)cobalt-(III) complexes, (+)-$[Co(en)_3]I_3$ and (−)-$[Co(en)_3]I_3$, are synthesized and prepared using standard methods.[31] Racemic mixture solutions of these enantiomers are also prepared. All solutions are prepared using a water:ethanol solvent mixture (1:1 by volume) and used immediately after preparation. Nonoptically active samples of $CoSO_4$ and $CoCl_2$ are also prepared and used as standards. All solvents are filtered before use (0.2 mm).

Results and Discussion

Circular Dichroism Signal. A half-wave plate in one of the input pump beams allows selection of the type of grating that is generated in the sample, either intensity, polarization, or a combination of the two. Data collection consists of monitoring the signal intensities for different samples while changing between gratings (i.e., rotating the half-wave plate). The ratio of the signal intensity from the polarization grating scheme (i.e., crossed pump polarizations) and the signal intensity from the intensity grating scheme (i.e., parallel pump polarizations) is the main focus for each individual sample. This ratio is more meaningful than comparing polarization grating signal intensities, since this ratio is immune to day-to-day experimental variations (e.g., laser power, optical alignment, etc.). Ratio comparison between chiral and nonchiral samples is the superior method to verify that the scattered signals truly result from circular dichroism effects and not from polarization impurities.

TABLE 1: Theoretical and Experimental Results of Circular Dichroism Measurements Using Circular Dichroism-Induced Thermal Gratings

	theoretical values		experimental values	
sample	dissymmety ratio	rotation angle, deg	dissymmety ratio	rotation angle, deg
(+)-$Co(en)_3^{3+}$	7.4×10^{-3}	+0.41	5.1×10^{-3}	+0.4
(−)-$Co(en)_3^{3+}$	-7.4×10^{-3}	−0.41	6.2×10^{-3}	−0.5

When the input pump beams have parallel linear polarizations, strong equally intense FWM signal beams are observed for the three equivalently concentrated $Co(en)_3^{3+}$ samples. These signals are expected to be identical for these solutions, since the resultant field in the beam crossover zone that creates the intensity-induced thermal grating has an unvarying polarization. However, when the two argon ion laser pump beams are crossed polarized, the results are different. In this case, a polarization grating is formed where the resultant field across the grating changes in polarization as described earlier. When these three samples are probed in this configuration, signal beams are observed only for the (+)-$Co(en)_3^{3+}$ and (−)-$Co(en)_3^{3+}$ solutions. As expected, no signal is detected for the racemic mixture. Also tested are samples of $CoSO_4$ and $CoCl_2$. These compounds absorb similarly to $Co(en)_3^{3+}$ at the 488 nm argon ion laser excitation wavelength, but they are not optically active. Strong FWM signals are observed for both samples when the pump beam polarizations are parallel, but as expected, no signals are detected for perpendicularly polarized pump beams above the scattered optical noise for these compounds with no optical activity.

Table 1 compares calculated and experimental dissymmetry ratios, $\Delta\epsilon/\epsilon$, for the two $Co(en)_3^{3+}$ enantiomers. The calculated ratios are determined using $\epsilon = 81$ and $\Delta\epsilon = 0.6$ L cm^{-1} mol^{-1}. Both these values are experimentally measured for the solutions of $Co(en)_3^{3+}$ using commercial UV−vis absorption and CD spectrometers. The experimental dissymmetry ratios are determined using

$$\frac{\Delta\epsilon}{\epsilon} = \left(\frac{S_\perp}{S_\parallel}\right)^{1/2} \tag{5}$$

where $S_\perp$ and $S_\parallel$ are the signal intensities for perpendicular (polarization grating) and parallel (intensity grating) polarized pump beams, respectively. As shown in Table 1, the theoretical and experimental values are in good agreement. The discrepancy between the experimental and theoretical results can be attributed primarily to the difficulty involved in measuring $S_\perp$. Since this signal is very small, it is often eclipsed by stray probe laser light. The use of micropinhole spatial filtering can overcome this problem effectively and allows the signal to be measured more accurately.

Direct Determination of $\Delta\epsilon/\epsilon$ by Grating Interference. As described earlier, it is possible to distinguish between different enantiomers by "mixing" a CD-induced thermal grating and an intensity-induced thermal grating. In our experiments the intensity grating is produced by placing a quarter-wave retardation plate in one of the pump beams. With the pump-beam polarizations crossed and the quarter-wave plate inserted with its optic axis parallel to the pump polarization, the FWM signal remains essentially unchanged. Upon a small rotation of the wave plate in one direction, the signal intensity drops to the

observed base line. At this point, the phase-shifted IGTG is 180° out of phase with the CDTG, and scattering from a thermal grating is minimized as described in Figure 4. If the wave plate is rotated an equal amount in the opposite direction relative to the optic axis, the observed signal rises, indicating that the IGTG is constructively interfering with the CDTG. When the sample is changed to the opposing enantiomer, the polarizations reverse. An equal but opposite rotation is required to minimize the signal.

The magnitude and sign of the quarter-wave plate rotation that is required to quench the CDTG can be calculated using eq 4. Table 1 lists the calculated rotation angles as well as the experimentally observed results for the two enantiomers studied. The theoretical and experimental values are again in good agreement. When a pulsed laser is used as the excitation source, as described by Terazima,[26] the potential for sensitive time-resolved CD measurements exist, since the time scale and resolution of the experiment are limited only by the pulse width of the laser system employed.

Future Work. Although the polarization-grating DFWM-CD method described in this work looks similar to the thermal-grating DFWM-CD technique reported previously,[19] there are some interesting and significant differences and advantages. A fundamental difference is that with this method the CD signal is on a true zero background, and it is not based on subtraction modulation techniques to derive the signal, since the signal is generated only if a chiral sample is present. This basic distinction therefore eliminates the need for any type of polarization modulation in the experimental setup, thereby dramatically simplifying CD measurements. Both thermal grating DFWM-CD and polarization grating DFWM-CD methods allow effective use of short path length sample cells and ultrasmall probe volumes, because the probe light comes from a laser and can be tightly focused. Hence, they offer effective and convenient interface to many chemical separation techniques (e.g., liquid chromatography or capillary electrophoresis). Although CD measurements with this polarization grating DFWM-CD technique are reliable and straightforward, stray probe laser light and polarization impurity problems can still obscure the signal. When measuring very small CD values; this background noise problem could become significant, since the measured signal has a quadratic dependence on the $\Delta\epsilon/\epsilon$ ratio. Further investigations are underway to improve the technique by combining this method and that described previously.[18] By strategically combining polarization gratings and intensity gratings using a dynamic polarization device (such as a photoelastic modulator), it should be possible to "amplify" the CD response similar to that done in heterodyne techniques used in Raman and frequency modulation spectroscopic methods. This grating combination would entail modulating between the situations shown in Figure 3c,d. This new scheme is currently being developed for CD detection in the ultraviolet region using pulsed laser excitation and will be reported in the near future.

Acknowledgment. We gratefully acknowledge partial support of this work from Sandia National Laboratories Office of Laboratory Directed Research and Development and the National Institute of General Medical Sciences, the National Institutes of Health under Grant 5-R01-GM41032. J. A. Nunes thanks the United States Department of Energy for an AWU-DOE Graduate Fellowship. The authors thank Dr. Skip Williams for helpful discussions and John Laroco for technical assistance.

References and Notes

(1) Eichler, H. J.; Gunter, P.; Pohl, D. W. *Laser-Induced Dynamic Gratings*; Springer-Verlag: Berlin, 1986.
(2) Farrow, R. L.; Rakestraw, D. J. *Science* **1992**, *257*, 1894−1900.
(3) Tong, W. G.; Chen, D. A. *Appl. Spectrosc.* **1987**, *41*, 586−590.
(4) Chen, D. A.; Tong, W. G. *J. Anal. Atom. Spectrom.* **1988**, *3*, 531−535.
(5) Wu, Z.; Tong, W. G. *Spectrochim. Acta* **1992**, *47B*, 449−457.
(6) Tong, W. G.; Andrews, J. M.; Wu, Z. *Anal. Chem.* **1987**, *59*, 896−899.
(7) Andrews, J. M.; Tong, W. G. *Spectrochim. Acta* **1989**, *44B*, 101−107.
(8) Andrews, J. M.; Weed, K. M.; Tong, W. G. *Appl. Spectrosc.* **1991**, *45*, 697−700.
(9) Wu, Z.; Tong, W. G. *Anal. Chem.* **1991**, *63*, 899−903.
(10) Wu, Z.; Tong, W. G. *Anal. Chem.* **1989**, *61*, 998−1001.
(11) Wu, Z.; Tong, W. G. *Anal. Chem.* **1991**, *63*, 1943−1947.
(12) Wu, Z.; Tong, W. G. *Anal. Chem.* **1993**, *65*, 112−117.
(13) Buntine, M. A.; Chandler, D. W.; Hayden, C. C. *J. Chem. Phys.* **1992**, *97*, 707−710.
(14) Gray, J. A.; Goldsmith, J. E. M.; Trebino, R. *Opt. Lett.* **1993**, *18*, 444−446.
(15) Harris, J. M.; Pelletier, M. J.; Thorshelm, H. R. *Anal. Chem.* **1982**, *54*, 239−242.
(16) Harris, J. M.; Pelletier, M. J. *Anal. Chem.* **1983**, *55*, 1537−1543.
(17) Butenhoff, T. J.; Rohlfing, E. A. *J. Chem. Phys.* **1992**, *97*, 1595−1602.
(18) Nunes, J. A.; Tong, W. G. *Anal. Chem.* **1993**, *65*, 2990−2994.
(19) Purdie, N.; Swallows, K. A. *Anal. Chem.* **1989**, *61*, 77A−89A.
(20) Nakanishi, K.; Kuroyanagi, M.; Nambu, H.; Oltz, E. M.; Takeda, R.; Verdine, G. L.; Zask, A. *Pure Appl. Chem.* **1984**, *56*, 1031−1048.
(21) Carrara, E. A.; Gavotti, C.; Catasti, P.; Nozza, F.; Berutti Bergotto, L. L.; Nicolini, C. A. *Arch. Biochem. Biophys.* **1992**, *294*, 107−114.
(22) Drake, A. F.; Gould, J. M.; Mason, S. F. *J. Chromatogr.* **1980**, *202*, 239−245.
(23) Westwood, S. A.; Games, D. E.; Sheen, L. *J. Chromatogr.* **1981**, *204*, 103−107.
(24) Premuzic, E. T.; Gaffney, J. S. *J. Chromatogr.* **1983**, *262*, 321−327.
(25) Nunes, J. A.; Tong, W. G.; Chandler, D. W.; Rahn, L. A. Sandia Report, SAND95-8221, UC-1409, 1995.
(26) Terazima, M. *J. Phys. Chem.* **1995**, *99*, 1834−1836.
(27) Meyers, A. B.; Hochstrasser, R. M. *IEEE J. Quantum Electron.* **1986**, *QE-22*, 1482.
(28) Fourkas, J. T.; Trebino, R.; Fayer, M. D. *J. Chem. Phys.* **1992**, *97*, 69−77.
(29) Moharam, M. G.; Gaylord, T. K.; Magnusson, R. *Opt. Commun.* **1980**, *32*, 19−23.
(30) Neyer, D. W.; Nunes, J. A.; Tong, W. G.; Rahn, L. A.; Chandler, D. W. Manuscript in preparation.
(31) Angelici, R. J. *Synthesis and Techniques in Inorganic Chemistry*, 2nd ed.; W. B. Saunders: Philadelphia, PA, 1977.